JEMMME (Journal of Energy, Mechanical, Material, and Manufacturing Engineering)
Vol.7, No. 1, 2022

ISSN 2541-6332 | e-ISSN 2548-4281
Journal homepage: http://ejournal.umm.ac.id/index.php/JEMMME

On Vehicle Stabilization Under Saturation Constraints by Linear Quadratic Regulator

Vania Katherine Mulia[a], Djati Wibowo Djamari[b], Ibham Veza[c] Ignatius Pulung Nurprasetio[d],
[a,b] Integrated Vehicle Research and Design Center
Mechanical Engineering Department
Faculty of Engineering and Technology
Sampoerna University
Jakarta 12780, Indonesia

[C] Faculty of Mechanical Engineering
Universiti Teknikal Malaysia Melaka
Hang Tuah Jaya, 76100 Durian Tunggal, Melaka, Malaysia

[d] Faculty of Mechanical and Aerospace Engineering
Institut Teknologi Bandung
Ganesha 10, Bandung 40132, Indonesia
(corresponding author)
e-mail: ipn@ftmd.itb.ac.id

Abstract

The stability of a four-wheel vehicle is an issue widely discussed. As an effort to reduce accidents involving four-wheel vehicles, many studies have been conducted to develop a vehicle stability control system. So far, all studies utilize vehicle lateral dynamics model as the reference to derive the desired states. However, defining the desired states using steady-state cornering values may yield instability due to changes in tire cornering stiffness. This paper proposes a simple vehicle stability control system that could stabilize the vehicle and allow tracking of a desired state under the case of vehicle instability due to reduced rear tire cornering stiffness. The controllers are designed using Linear Quadratic Regulator (LQR) technique and combined with the servo control system to track a reference state. Simulations are performed in MATLAB to validate the controller's performance with and without controller constraint. Results show that the controller successfully stabilizes the vehicle and tracks the desired state.

Keywords*: vehicle stability control; Linear Quadratic Regulator (LQR)*

1. INTRODUCTION

Road safety has remained as one of the most discussed issues, as the World Health Organization (WHO) reports that, as of 2021, the number of deaths by road accidents reaches 1.3 million per year (1). Furthermore, WHO also reports in the Global Status Report on Road Safety 2018 that car occupants (or four-wheeled vehicles in general) contribute to 29% of all road traffic fatalities (2). To reduce this number, vehicle stability control (VSC) becomes one of the solutions. According to a statistical analysis, VSC can minimize vehicle involvement in multivehicle frontal crashes by up to 11.8 percent and single-vehicle crashes by up to 52.6 percent (3). Many studies have been done to introduce better control systems to improve vehicle yaw stability. A review of various vehicle control systems, as well as their benefits and drawbacks, is presented in (4). While most control strategies demonstrate robustness against uncertainties owing to vehicle characteristics, there are various drawbacks, most of which are linked to online optimization, transient response not considered, and implementation difficulty.

In general, there are two types of vehicle stability control, which are active steering (AS) and direct yaw control (DYC). Active steering works by providing a corrective angle to the tires in response to the driver's steering command and the vehicle states (4). Many control strategies, such as Sliding Mode Control (SMC) (5), H_∞, Model Predictive Control (MPC), Quantitative Feedback Theory (QFT), Fuzzy-Logic Control (FLC), and passivity-based adaptive nonlinear control, have been developed for active steering systems that are robust to uncertainty (4). A study in (5) presents a strategy to integrate AS with active roll control to improve handling and rollover stability. The active steering control is designed using sliding mode control based on the 2-DoF (bicycle) model. Simulation performed in CarSim for J-turn and lane change maneuvers shows that the sliding mode control can achieve the desired conditions with less control effort. Moreover, the control effort is also smoother. The disadvantage of active steering is that it is significantly influenced by tire nonlinearity and tire saturation when it comes to tire slip angles (4).

Direct yaw moment control (DYC) discusses more on vehicle stability control system. DYC works by adding a yaw moment by applying driving or braking torque to the left or right tire. Based on the controller output, DYC can be classified as active differential braking (ADB) or active torque disturbance (ATD) (4). The disadvantage of ADB is that excessive braking slows down the vehicle's speed. When it comes to ATD, if the road friction coefficient is too low or the vehicle's velocity is too high, the system may fail to provide appropriate yaw moment (4).

Several robust control algorithms for DYC systems have also been developed, including sliding mode control (SMC) (6,7), Linear Quadratic Regulator (LQR) (8,9), and H_∞ (10). In addition, DYC takes over a more varying applications, especially in the development of stability control for electric vehicle (EV) (6,7,9,10). A study in (6) focuses on resolving the chattering problems associated with in-wheel EV by designing a second-order sliding controller, and simulations using CarSim for double lane change maneuvers show that the proposed controller not only improves the stability of the vehicle, but also reduces the problem of heavy chattering. Meanwhile, in (7), the authors initially explore the influence of variation in loading conditions and the effect of ignoring changes in inertial parameters for an ultra-lightweight solar-electric vehicle before proposing a sliding mode controller to improve yaw stability. In (8), the authors propose a novel control algorithm of DYC based on a hierarchical control strategy in which the upper controller uses LQR that contains feedback control and feed-forward control, and simulations executed on the Hardware-in-the-Loop (HIL) simulation platform prove that the proposed controller is more effective in reducing control delay or overshoot and taking account for tire forces. In (9), the authors propose a combined lane keeping and DYC controller for intelligent EV using LQR, in which the inherent time delay and data dropouts are incorporated into the vehicle's lateral dynamics, and the controller is proven effective through simulations using Adams-Simulink joint platform for single and double lane-change maneuvers. In (10), the authors design a controller for four-wheel independently actuated (FWIA) electric ground vehicles considering the tire force saturations using linear parameter-varying (LPV) based robust H_∞ controller, and it is successfully simulated using CarSim for single lane-changing and J-turn maneuvers with an external disturbance in the form of hard brake.

Further studies have attempted to combine active steering and DYC to overcome the weakness of both controllers and achieve optimum control effort (11,12). In (11), the authors combine DYC with active rear steering through an upper and lower-level controller. The upper-level controller generates the required yaw moment and rear steering angle using sliding mode controller based on a 2-DoF vehicle model while the lower-level controller distributes the yaw moment to the four wheels using a braking torque distribution scheme. In (12), the authors combine DYC with active front steering using fuzzy programming, which produces a weighted combination of the two control inputs. Furthermore, the controller utilizes Unscented Kalman Filter (UKF) for the estimation of the required vehicle states and parameters from the measured data. Both studies prove through simulations that the controllers successfully enhance the handling and stability of a vehicle.

So far, all studies mentioned above utilize vehicle lateral dynamics to model the system and take the steady-state solutions as the reference states. However, the

reference states from the steady-state solutions depend on the vehicle parameters such as the tire cornering stiffness which heavily affects whether the vehicle is in normal steer, understeer, or oversteer (13). A study in (14) shows that a vehicle can become unstable when the rear tire cornering stiffness is reduced. There are many factors affecting the cornering stiffness of a tire, such as tire size, type, treads (15), inflation pressure (16,17), and vertical load (18).

This paper aims to design simple controllers to improve the yaw stability under such condition. This paper discusses two types of controllers, both designed using LQR. The first controller focuses only to stabilize the vehicle handling system. The second controller aims to track a reference state, which is the desired yaw rate, and it is designed using the servo system to create the closed-loop state space system before applying the LQR technique. Furthermore, this paper also provides a new approach to define the desired states, using the Ackermann Geometry to calculate the yaw rate at normal steering.

The paper is organized as follows: it is started with the first section that outlines the introduction, literature survey, and objective, followed by the second section on methodology, the third section on simulation results and discussion, before in section four the conclusions are explained.

2. METHODOLOGY

2.1 Modeling of Vehicle Handling

To design the controller, the handling system of a four-wheel vehicle must be modelled mathematically. This mathematical model is an expansion of the bicycle model, with the addition of braking forces as the controller output (11–13). The free-body diagram (FBD) of the four-wheel vehicle model is depicted in **Error! Reference source not found.** while the parameters are elaborated in Table 1.

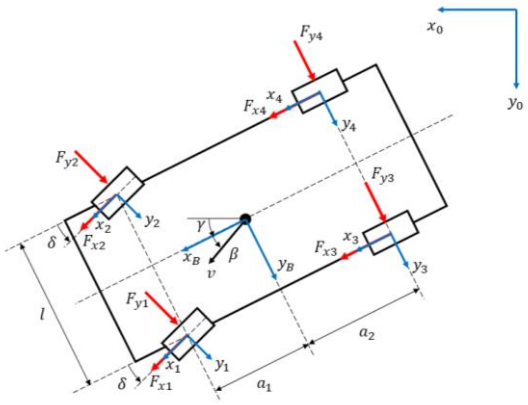

Figure 1. FBD of the four-wheel vehicle model

Table 1. Parameters used in vehicle handling system modelling

Symbol	Description
β	Side-slip angle
γ	Yaw angle
ω	Yaw rate
m	Vehicle mass
Θ	Vehicle mass moment of inertia about the vertical axis
c_{s1}	Cornering stiffness of front tire
c_{s2}	Cornering stiffness of rear tire
a_1	Distance between the center of mass and front tire axle
a_2	Distance between the center of mass and rear tire axle
v	Velocity of the vehicle
δ	Steering angle

In the modelling of the handling system, small angle approximation is applied to yaw velocity of the vehicle $\dot{\gamma}$, the side slip angle β, and the steering angle δ (10,13). In addition, since the side slip angle is the smaller angle between the velocity vector and the vehicle longitudinal axis, the longitudinal velocity may be approximated as:

$$v \sin \beta = |v|\beta \tag{1}$$

Equation of motion (using small angle approximation for δ and β) may be expressed as:

$$m\left(v\omega + |v|\dot{\beta}\right) = F_{yf} + F_{yr} \tag{2}$$

and the angular motion becomes

$$\Theta\dot{\omega} = a_1 F_{yf} - a_2 F_{yr} + M_z \tag{3}$$

where $\omega = \dot{\gamma}$, F_{yf} is the sum of front tires lateral forces, which can be expanded to

$$F_{yf} = F_{y1} + F_{y2} \tag{4}$$

F_{yr} is the sum of rear tires lateral forces, which can also be expanded to

$$F_{yr} = F_{y3} + F_{y4} \tag{5}$$

and M_z is the external yaw moment, which is the control input.

The tire lateral forces may be expressed as a linear function

$$F_y = c_s s_y \tag{6}$$

where s_y is the lateral slip. Using the small angle approximation, the lateral slip of front tire may be expressed as

$$s_{yf} = -\beta - \frac{a_1}{|v|}\omega + \frac{v}{|v|}\delta \tag{7}$$

and the lateral slip of the rear tire may be expressed as

$$s_{yr} = -\beta + \frac{a_2}{|v|}\omega \tag{8}$$

Deriving the equations of motion yielded a state space formulation (10) expressed by

$$\dot{\boldsymbol{x}} = \boldsymbol{A}\boldsymbol{x} + \boldsymbol{B_1}u_1 + \boldsymbol{B_2}u_2 \tag{9}$$

in which

$$\boldsymbol{x} = \begin{bmatrix} \beta \\ \omega \end{bmatrix} \tag{10a}$$

$$\boldsymbol{A} = \begin{bmatrix} -\frac{c_{sf}+c_{sr}}{m|v|} & \frac{a_2c_{sr}-a_1c_{sf}}{m|v||v|} - \frac{v}{|v|} \\ \frac{a_2c_{sr}-a_1c_{sf}}{\Theta} & -\frac{a_1^2c_{sf}+a_2^2c_{sr}}{\Theta|v|} \end{bmatrix} \tag{10b}$$

$$\boldsymbol{B_1} = \begin{bmatrix} 0 \\ \frac{1}{\Theta} \end{bmatrix} \tag{10c}$$

$$\boldsymbol{B_2} = \begin{bmatrix} \frac{v}{|v|}\frac{c_{sf}}{m|v|} \\ \frac{v}{|v|}\frac{a_1c_{sf}}{\Theta} \end{bmatrix} \tag{10d}$$

$$u_1 = M_z \tag{10e}$$

$$u_2 = \delta \tag{10f}$$

M_z can be defined from the longitudinal forces of each tire (10), expressed as:

$$M_z = \sum_{i=1}^{4}(-1)^i F_{xi}\frac{l}{2} \tag{11}$$

The model also uses the TMEasy tire model to define the tire forces (19). This model is used due to its simplicity. This model approximates that the lateral force of the tire is proportional to the wheel load and the lateral slip. This relationship can be expressed mathematically as

$$F_y = kF_zs_y \tag{12}$$

where F_y is the lateral force of the tire, F_z is the vertical wheel load, s_y is the lateral slip, and k is a constant representing the tire properties such as tire tread size, tread stiffness, tire loaded radius, and tire radial stiffness. This relation holds for small slip condition; in this condition, all treads stick to the road. The vertical load of each tire can be calculated by distributing the vehicle's weight (13) using the formula

$$F_{zf} = \left(\frac{a_2}{a_1+a_2}\right)mg \tag{13}$$

$$F_{zr} = \left(\frac{a_1}{a_1+a_2}\right)mg \tag{14}$$

where F_{zf} and F_{zr} are the front and rear vertical wheel load, respectively.

2.2 Controller Design

The objective of the controller is to stabilize the vehicle and to track a reference state (servo purpose). Since u_1 is the control input, as the first check, the sufficient condition to design the controller is the controllability of the pair $\boldsymbol{A}$ and $\boldsymbol{B_1}$. The controllability matrix for $(\boldsymbol{A}, \boldsymbol{B_1})$ may be assessed by looking at the rank of the following matrix (20):

$$[\boldsymbol{B_1} \quad \boldsymbol{AB_1}] = \begin{bmatrix} 0 & \left(\frac{a_2c_{sr}-a_1c_{sf}}{m|v||v|} - \frac{v}{|v|}\right)\frac{1}{\Theta} \\ \frac{1}{\Theta} & \left(-\frac{a_1^2c_{sf}+a_2^2c_{sr}}{\Theta|v|}\right)\frac{1}{\Theta} \end{bmatrix} \tag{15}$$

The system will be uncontrollable, i.e., matrix (15) is not full rank, if:

$$\left(\frac{a_2c_{sr}-a_1c_{sf}}{m|v||v|} - \frac{v}{|v|}\right)\frac{1}{\Theta} = 0 \tag{16}$$

Since $\frac{1}{\Theta} \neq 0$, equation (16) may be written as:

$$\frac{a_2c_{sr}-a_1c_{sf}}{m|v||v|} - \frac{v}{|v|} = 0 \tag{17}$$

However, notice that satisfying this condition makes the state matrix A becomes

$$\boldsymbol{A} = \begin{bmatrix} -\frac{c_{sf}+c_{sr}}{m|v|} & 0 \\ \frac{a_2c_{sr}-a_1c_{sf}}{\Theta} & -\frac{a_1^2c_{sf}+a_2^2c_{sr}}{\Theta|v|} \end{bmatrix} \tag{18}$$

and by noting that it is a lower triangular matrix, the eigenvalues of this matrix are

$$\lambda_1 = -\frac{c_{sf}+c_{sr}}{m|v|},\ \lambda_2 = -\frac{a_1^2c_{sf}+a_2^2c_{sr}}{\Theta|v|} \tag{19}$$

which will always have negative real values. Therefore, the system is always stable. Since the system is stable even when it is uncontrollable, it can be concluded that the system is always stabilizable, which is the necessary and sufficient condition for the existence of stabilizing feedback matrix.

To stabilize the vehicle, a controller is designed using Linear Quadratic Regulator (LQR). Using this technique, the control input may be expressed as

$$\boldsymbol{u} = -\boldsymbol{Kx} \tag{20}$$

in which the matrix K is designed to minimize the following performance index

$$J = \int_0^\infty (\boldsymbol{x}^T\boldsymbol{Q}\boldsymbol{x} + \boldsymbol{u}^T\boldsymbol{R}\boldsymbol{u})\, dt \tag{21}$$

where $\boldsymbol{Q}$ and $\boldsymbol{R}$ determine the relative importance of the error and the expenditure of the control effort (20).

In the case of the state space system expressed in equation (9), since the control input u_1 corresponds to the matrix $\boldsymbol{B_1}$, the value of $\boldsymbol{K}$ can be determined from

$$\boldsymbol{K} = \boldsymbol{R}^{-1}\boldsymbol{B_1}^T\boldsymbol{P} \tag{22}$$

and the matrix $\boldsymbol{P}$ is determined by solving the Riccati equation (20) defined by

$$\boldsymbol{A}^T\boldsymbol{P} + \boldsymbol{P}\boldsymbol{A} - \boldsymbol{P}\boldsymbol{B_1}\boldsymbol{R}^{-1}\boldsymbol{B_1}^T\boldsymbol{P} + \boldsymbol{Q} = \boldsymbol{0} \tag{23}$$

In most situations, however, stabilizing the vehicle is not sufficient to ensure the safety of the driver and/or passengers. Even though a vehicle is stabilized, there are still possibilities that the vehicle experience oversteering, which is still considered dangerous. To further correct this situation, a second type of controller is designed with the goal of not only to stabilize, but also to track desired states associated with neutral steer condition.

The desired states can be derived using the Ackermann Geometry, as it reflects the condition of neutral steer during cornering (13). The schematic of Ackermann Geometry is depicted in Figure 1. As there are two states involved in the state space system in

equation (10a), which are the slip angle β and the yaw rate ω, analytically the desired value for both states can be found using the Ackermann geometry. However, only the yaw rate ω is used as the desired state for the controller since a servo system can only accept one desired state.

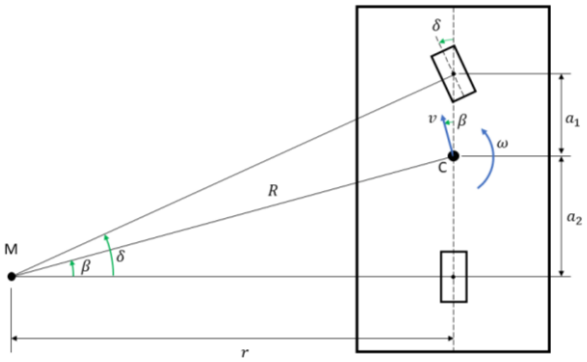

Figure 1 Ackermann geometry of a bicycle model

Using trigonometry on the steering angle δ,

$$\tan \delta = \frac{a_1+a_2}{r} \tag{24}$$

In the mathematical modelling of vehicle handling system, again small angle approximation is used for the steering angle δ. For consistency, the same approximation applies to the Ackermann geometry. Applying the small angle approximation yields

$$\tan \delta \approx \delta = \frac{a_1+a_2}{r} \tag{25}$$

$$r = \frac{a_1+a_2}{\delta} \tag{26}$$

The cornering radius R, which is the distance from the curvature center point to the vehicle's center of mass, based on Figure 1, can be calculated as

$$R = \sqrt{r^2 + a_2^2} = \sqrt{\left(\frac{a_1+a_2}{\delta}\right)^2 + a_2^2} \tag{27}$$

$$R = \sqrt{\frac{(a_1+a_2)^2+a_2^2\delta^2}{\delta^2}} = \frac{1}{\delta}\sqrt{(a_1+a_2)^2 + a_2^2\delta^2} \tag{28}$$

The desired yaw rate is found from the vehicle's kinematics, expressed as

$$\omega = \frac{v}{R} \tag{29}$$

$$\omega = \frac{v\delta}{\sqrt{(a_1+a_2)^2+a_2^2\delta^2}} \tag{30}$$

To track the desired states, the controller was designed using servo control combined with LQR (20). Since the servo control only allows one reference state, the desired yaw rate expressed in equation (30) is used as the reference state. The system still follows from equation (9) and

$$y = \boldsymbol{Cx} \tag{31}$$

where

$$C = [0 \quad 1] \tag{32}$$

Taking the yaw rate ω as the desired state yields $y_d = \omega_d$. The error signal is then defined as

$$e(t) = y_d - y(t) = y_d - \boldsymbol{Cx} \tag{33}$$

The integral of error is defined as

$$v(t) = \int_0^t e(t) \tag{34}$$

$$\dot{v}(t) = e(t) = y_d - \boldsymbol{C}\boldsymbol{x}(t) \tag{35}$$

Combining the dynamics of $\boldsymbol{x}$ and v, the augmented state space system becomes

$$\begin{bmatrix}\dot{\boldsymbol{x}}\\ \dot{v}\end{bmatrix} = \begin{bmatrix}\boldsymbol{A} & \boldsymbol{0}\\ -\boldsymbol{C} & 0\end{bmatrix}\begin{bmatrix}\boldsymbol{x(t)}\\ v(t)\end{bmatrix} + \begin{bmatrix}\boldsymbol{B_1}\\ 0\end{bmatrix}u_1 + \begin{bmatrix}\boldsymbol{B_2}\\ 0\end{bmatrix}u_2 + \begin{bmatrix}\boldsymbol{0}\\ 1\end{bmatrix}y_d \tag{36}$$

Let us define the control input u_1 as

$$u_1 = -\boldsymbol{K_1}\boldsymbol{x}(t) - K_2 v(t) \tag{37}$$

in which u_1 is a scalar, $\boldsymbol{K_1}$ is a 1×2 feedback matrix, and K_2 is a scalar feedback term. The resulting closed loop system will be

$$\begin{bmatrix}\dot{\boldsymbol{x}}\\ \dot{v}\end{bmatrix} = \begin{bmatrix}\boldsymbol{A} - \boldsymbol{B_1}\boldsymbol{K_1} & -\boldsymbol{B_1}K_2\\ -\boldsymbol{C} & 0\end{bmatrix}\begin{bmatrix}\boldsymbol{x(t)}\\ v(t)\end{bmatrix} + \begin{bmatrix}\boldsymbol{B_2}\\ 0\end{bmatrix}u_2 + \begin{bmatrix}\boldsymbol{0}\\ 1\end{bmatrix}y_d \tag{38}$$

It may be rewritten as

$$\hat{\dot{\boldsymbol{x}}} = (\widehat{\boldsymbol{A}} - \widehat{\boldsymbol{B}}_{\boldsymbol{1}}\boldsymbol{K})\hat{\boldsymbol{x}} + \widehat{\boldsymbol{B}}_{\boldsymbol{2}}\hat{\boldsymbol{u}}_{\boldsymbol{2}} \tag{39}$$

in which

$$\hat{\boldsymbol{x}} = \begin{bmatrix}\boldsymbol{x(t)}\\ v(t)\end{bmatrix} \tag{40a}$$

$$\widehat{\boldsymbol{A}} = \begin{bmatrix}\boldsymbol{A} & \boldsymbol{0}\\ -\boldsymbol{C} & 0\end{bmatrix} \tag{40b}$$

$$\widehat{\boldsymbol{B}}_{\boldsymbol{1}} = \begin{bmatrix}\boldsymbol{B_1}\\ 0\end{bmatrix} \tag{40c}$$

$$\boldsymbol{K} = [\boldsymbol{K_1} \quad K_2] \tag{40d}$$

$$\widehat{\boldsymbol{B}}_{\boldsymbol{2}} = \begin{bmatrix}\boldsymbol{B_2} & \boldsymbol{0}\\ 0 & 1\end{bmatrix} \tag{40e}$$

$$\hat{\boldsymbol{u}}_{\boldsymbol{2}} = \begin{bmatrix}u_2\\ y_d\end{bmatrix} \tag{40f}$$

When the servo control is combined with the LQR, equation (36) becomes the augmented state space that is the input for the LQR.

The yaw moment that the controller can provide has a limit. Since the yaw moment is created by uneven braking forces, there is a maximum braking force value depending on the tire friction force, which is quantified by the friction coefficient. It is necessary that the braking force on a tire does not exceed the tire friction force such that no longitudinal slip occurs. This constraint was later added into the simulation for the reference-tracking controller to show how the constraint may affect the system. Let the upper and lower limit

of the control input be denoted as $u_{max} = u^*$ and $u_{min} = -u^*$, respectively. The controller with the constraint imposed may be expressed as

$$u_1 = \begin{matrix} u_1, if\ |u_1| < u^* \\ u^*, if\ |u_1| > u^* \end{matrix} \quad (41)$$

in which u_1 is given by (37).

The simulation was performed using MATLAB, with the parameters listed in Table 2. As for the rear tire cornering stiffness, the multiplier constant k_r was set as two step functions, as seen in

Figure 2. This condition shows that initially, the value of k_r is the same as k_f in Table 2, or in other words, the front and rear tires are identical. However, at $t = 5$ seconds, the value of k_r drops to just 0.4 times its initial value, making the vehicle inherently unstable. At this state, the controller should be triggered to provide control input to the handling system, and the simulation should show how the controller prevents instability, either by stabilizing the yaw rate or by tracking the desired yaw rate.

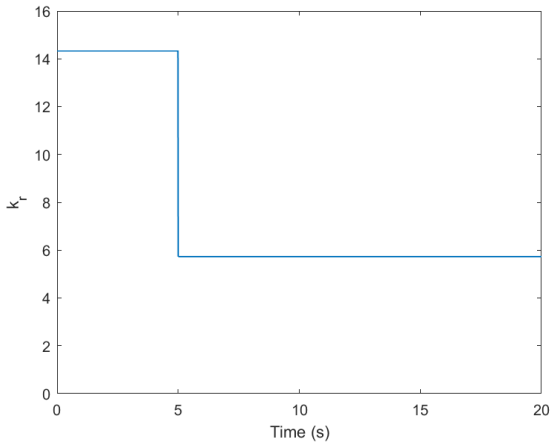

Figure 2. Rear tire cornering stiffness multiplier

Table 2. Simulation Parameters

Symbol	Description	Value
m	Mass of the vehicle	1600 kg
Θ	Mass moment of inertia of the vehicle	1058.57 kg.m^2
k_f	Front tire stiffness multiplier constant	14.33
a_1	Distance between front tire axle and center of mass	1.2 m
a_2	Distance between rear tire axle and center of mass	1.45 m
v	Velocity of the vehicle	80 km/h (22.22 m/s)
δ	Constant steering angle	0.5 rad

3. RESULTS AND DISCUSSIONS

3.1 Controller Without Constraint

Prior to designing the controller, the controllability and/or stabilizability of the state space system were checked. The sufficient condition was that the system is stabilizable. Once this condition is ensured, the controllers could be designed. All controllers were designed using LQR.

The controller was also designed so that it only produces control input to the vehicle system when the yaw rate exceeds a tolerance of 5% of the desired yaw rate. The value of 5% was chosen arbitrarily for this simulation, however, in a real-life application, this number can be tuned according to the driver's convenience.

For the stabilizing controller, the simulation result can be seen in Figure 3. The system becomes unstable after 5 seconds, indicated by the red dashed curve approaching a large value. The simulation also shows that the controller can stabilize the system, indicated by the black curve approaching a steady-state value. This value, however, is still higher than the desired yaw rate, which is the yaw rate when the vehicle is in normal steer. This means that the vehicle is still in oversteer. Thus, in real life application, there are still some risks attributed to this controller. The yaw moment generated by the controller can be seen in Figure 4. For this controller, the yaw moment generated by the controller rises to a certain value and then stays constant for the rest of the simulation time.

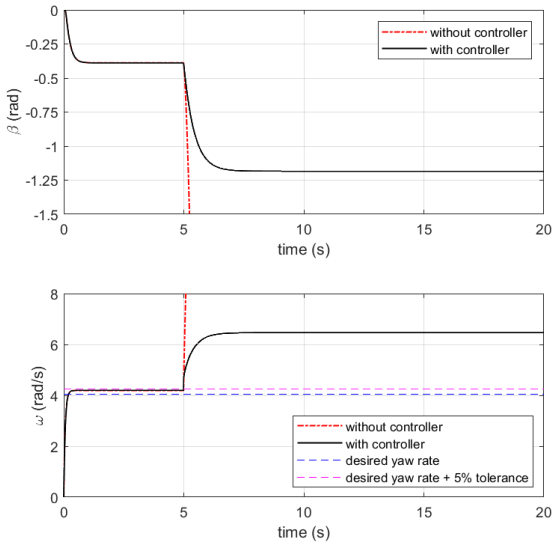

Figure 3. Simulation result for stabilizing controller with no constraint

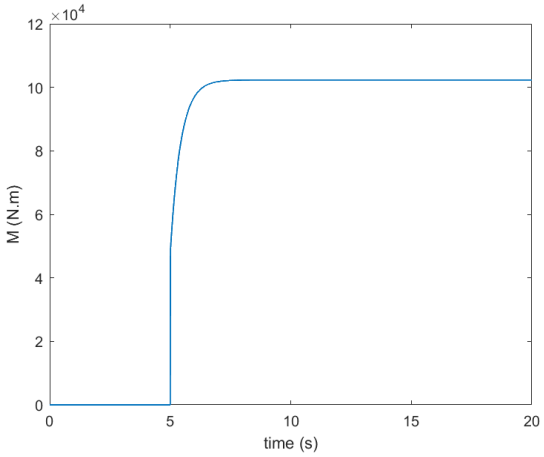

Figure 4. Yaw moment generated by stabilizing controller with no constraint

For the reference-tracking controller, the simulation result can be seen in Figure 5. With the addition of servo system, the controller now provides a control input that makes the yaw rate approaches the desired yaw rate, although achieving it at a slower rate compared to the stabilizing controller. The system becomes a non-minimum phase system indicated by the existence of "overshoot" before both states reach a steady state value. The yaw moment produced by this controller can be seen in Figure 6. For this controller, the yaw moment rises to a maximum value and then slowly reducing to a certain steady-state value.

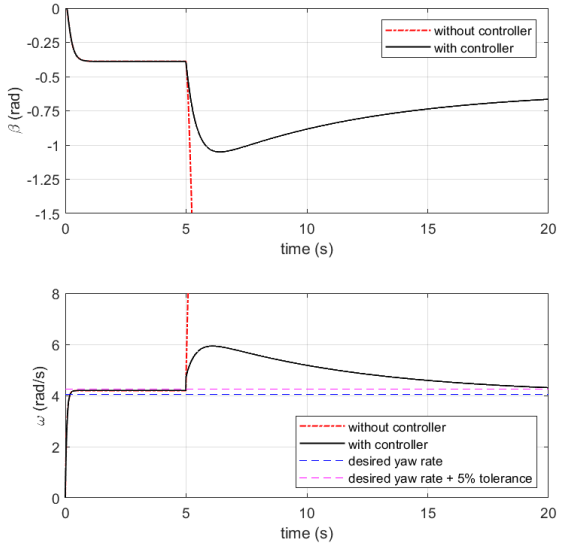

Figure 5. Simulation result for reference-tracking controller with no constraint

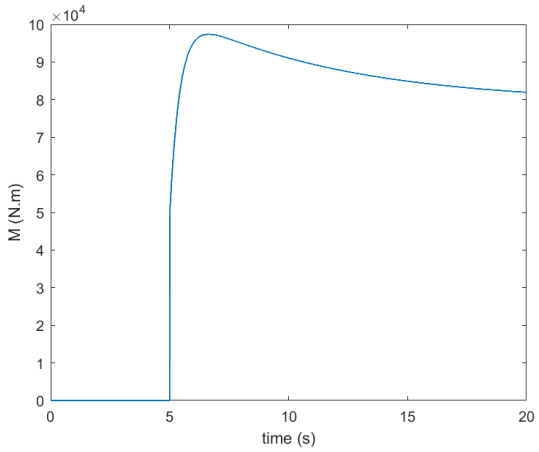

Figure 6. Yaw moment generated by reference-tracking controller with no constraint

3.2 Controller with Constraint

To apply the yaw rate constraint, additional lines of codes were added into the simulation that represents the saturation function given by (22). For the reference-tracking controller, there are several possible scenarios depending on the value of the yaw moment limit. When the limit is too low, the controller will be unable to produce the required yaw moment to track the reference state. There is also a scenario when the limit is slightly below the maximum yaw moment normally produced by the controller without constraint, however, the controller is still able to track the desired yaw rate. Figure 7 shows the simulation result for such case, and the yaw moment generated by the

controller can be seen in Figure 8. The red dashed line in Figure 8 indicates the yaw moment limit. When the yaw moment reaches the limit, the yaw moment value will remain constant for a certain period. This yaw moment, despite not as high as the maximum value for the case without constraint, is still enough to bring the yaw rate to the desired value. As the yaw rate is brought closer to the desired value, the required yaw moment decreases.

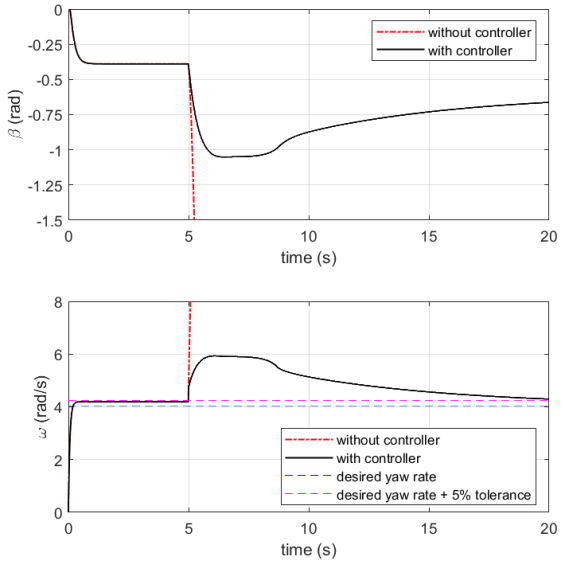

Figure 7. Simulation result for reference-tracking controller with constraint

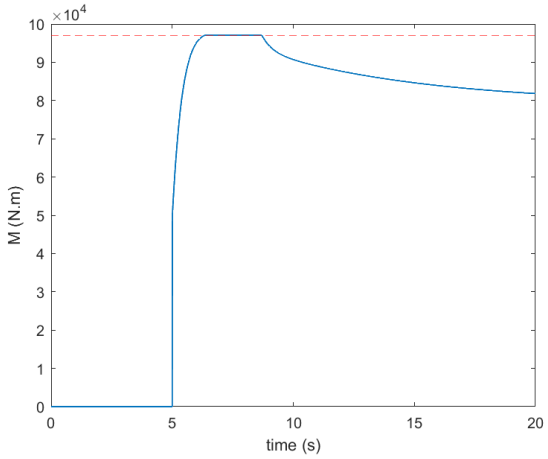

Figure 8. Yaw moment generated by reference-tracking controller with constraint

4. CONCLUSION

This paper proposes a vehicle stability control system to provide handling stability in cases of instability due to a sudden tire cornering stiffness change. Two types of controllers are designed in this paper, one to stabilize the vehicle and the second to track a desired yaw rate value based on the Ackermann Geometry. The controllers are successfully designed using LQR technique and combined with servo control system for reference-tracking. The controller's performance is simulated using MATLAB for cases with and without a controller constraint.

Simulation results show that the controllers successfully accomplish its purpose to stabilize and/or track the desired yaw rate. For the stabilizing controller, simulation results

show that the states approach a steady state value which validates the controller's performance. However, the yaw rate is still above that of the normal steer value. By designing the reference-tracking controller, the yaw rate may approach the desired value. Furthermore, the reference-tracking controller allows for controller constraint due to tire friction force.

As a future work, fine tuning of the controller parameters such as the desired state tolerance limit needs to be carried out. Furthermore, laboratory experiments with real or model vehicles need to be carried out to quantify the controller constraint and to validate the controller's performance.

ACKNOWLEDGEMENT

This research is funded by the Indonesia Endowment Fund for Education (LPDP) under Research and Innovation Program (RISPRO) for electric vehicle development with contract no. PRJ-85/LPDP/2020 and Center of Research and Community Service (CRCS) of Sampoerna University.

REFERENCES

1. World Health Organization. Road traffic injuries [Internet]. 2021 [cited 2021 Nov 5]. Available from: https://www.who.int/news-room/fact-sheets/detail/road-traffic-injuries
2. World Health Organization. Global Status Report on Road Safety 2018. Geneva; 2018.
3. Bahouth G. Real World Crash Evaluation of Vehicle Stability Control (VSC) Technology. Annu Proc / Assoc Adv Automot Med [Internet]. 2005 [cited 2021 Nov 5];49:19. Available from: /pmc/articles/PMC3217442/
4. Mousavinejad IE, Zhu Y, Vlacic L. Control strategies for improving ground vehicle stability: State-of-the-art review. 2015 10th Asian Control Conf Emerg Control Tech a Sustain World, ASCC 2015. 2015;
5. Saeedi MA. A new robust combined control system for improving manoeuvrability, lateral stability and rollover prevention of a vehicle. Proc Inst Mech Eng Part K J Multi-body Dyn. 2020;234(1):198–213.
6. Ding S, Liu L, Zheng WX. Sliding Mode Direct Yaw-Moment Control Design for In-Wheel Electric Vehicles. IEEE Trans Ind Electron. 2017 Aug 1;64(8):6752–62.
7. Lidfors Lindqvist A, Zhou S, Walker PD. Direct yaw moment control of an ultra-lightweight solar-electric passenger vehicle with variation in loading conditions. https://doi.org/101080/0042311420201853784 [Internet]. 2020 [cited 2022 May 31];60(4):1393–415. Available from: https://www.tandfonline.com/doi/abs/10.1080/00423114.2020.1853784
8. Li L, Jia G, Chen J, Zhu H, Cao D, Song J. A novel vehicle dynamics stability control algorithm based on the hierarchical strategy with constrain of nonlinear tyre forces. Veh Syst Dyn. 2015 Aug 3;53(8):1093–116.
9. Guo J, Luo Y, Hu C, Tao C, Li K. Robust Combined Lane Keeping and Direct Yaw Moment Control for Intelligent Electric Vehicles with Time Delay. Int J Automot Technol 2019 202 [Internet]. 2019 Mar 30 [cited 2022 May 31];20(2):289–96. Available from: https://link.springer.com/article/10.1007/s12239-019-0028-5
10. Wang R, Zhang H, Wang J, Yan F, Chen N. Robust lateral motion control of four-wheel independently actuated electric vehicles with tire force saturation consideration. J Franklin Inst [Internet]. 2015;352(2):645–68. Available from: http://dx.doi.org/10.1016/j.jfranklin.2014.09.019
11. Li B, Rakheja S, Feng Y. Enhancement of vehicle stability through integration of direct yaw moment and active rear steering. Proc Inst Mech Eng Part D J Automob Eng. 2016;230(6):830–40.
12. Mirzaeinejad H, Mirzaei M, Rafatnia S. A novel technique for optimal integration of active steering and differential braking with estimation to improve vehicle directional stability. ISA Trans. 2018;80(June):513–27.
13. Rill G, Castro AA. Road Vehicle Dynamics : Fundamentals and Modeling with MATLAB® [Internet]. 2nd ed. Road Vehicle Dynamics. Boca Raton: CRC Press;

2020 [cited 2022 Jun 1]. Available from: https://www.taylorfrancis.com/books/mono/10.1201/9780429244476/road-vehicle-dynamics-georg-rill-abel-arrieta-castro

14. Mulia VK, Endrasari F, Wibowo D, Veza I. Parametric Study of Factors Affecting Lateral Stability of a Public Transportation Vehicle. Int J Sustain Transp Technol. 2021 Oct 31;4(2):79–86.
15. Vorotovic GS, Rakicevic BB, Mitic SR, Stamenkovic DD. Determination of cornering stiffness through integration of a mathematical model and real vehicle exploitation parameters. FME Trans. 2013;41(1):66–71.
16. Singh KB. Vehicle sideslip angle estimation based on tire model adaptation. Electron. 2019;8(2):1–24.
17. Strigel A, Peckelsen U, Unrau H-J, Gauterin F. Estimation of feasible ranges of functional tire characteristics based on tire dimension, inflation pressure, and wheel load. Proc Inst Mech Eng Part D J Automob Eng [Internet]. 2019 Feb 22;233(14):3700–6. Available from: https://doi.org/10.1177/0954407019831575
18. El-Sayegh Z, El-Gindy M. Cornering characteristics of a truck tire on wet surface using finite element analysis and smoothed-particle hydrodynamics. Int J Dyn Control 2018 64 [Internet]. 2018 Feb 9 [cited 2021 Oct 15];6(4):1567–76. Available from: https://link.springer.com/article/10.1007/s40435-018-0403-5
19. Rill G. TMeasy–A Handling Tire Model based on a three-dimensional slip approach. In: Proceedings of the XXIII International Symposium on Dynamic of Vehicles on Roads and on Tracks (IAVSD 2013) [Internet]. 2013 [cited 2022 May 31]. Available from: https://www.researchgate.net/publication/317037031
20. Ogata K. Modern Control Engineering. 5th ed. Uppern Saddle River, NJ: Prentice Hall; 2010. 894 p.